Article

Understanding Atom Transfer Radical Polymerization: Effect of Ligand and Initiator Structures on the Equilibrium Constants

Wei Tang, Yungwan Kwak, Wade Braunecker, Nicolay V. Tsarevsky, Michelle L. Coote, and Krzysztof Matyjaszewski

J. Am. Chem. Soc., **2008**, 130 (32), 10702-10713 • DOI: 10.1021/ja802290a • Publication Date (Web): 19 July 2008

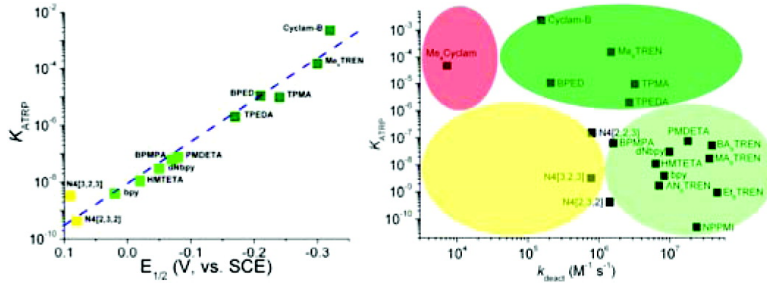

More About This Article

Additional resources and features associated with this article are available within the HTML version:

- Supporting Information
- Links to the 1 articles that cite this article, as of the time of this article download
- Access to high resolution figures
- Links to articles and content related to this article
- Copyright permission to reproduce figures and/or text from this article

View the Full Text HTML

Journal of the American Chemical Society is published by the American Chemical Society. 1155 Sixteenth Street N.W., Washington, DC 20036

J|A|C|S
ARTICLES

Published on Web 07/19/2008

Understanding Atom Transfer Radical Polymerization: Effect of Ligand and Initiator Structures on the Equilibrium Constants

Wei Tang,[†] Yungwan Kwak,[†] Wade Braunecker,[†] Nicolay V. Tsarevsky,[†] Michelle L. Coote,[‡] and Krzysztof Matyjaszewski*,[†]

Center for Macromolecular Engineering, Department of Chemistry, Carnegie Mellon University, 4400 Fifth Avenue, Pittsburgh, Pennsylvania 15213, and ARC Centre of Excellence for Free-Radical Chemistry and Biotechnology, Research School of Chemistry, Australian National University, Canberra ACT 0200, Australia

Received March 28, 2008; E-mail: km3b@andrew.cmu.edu

Abstract: Equilibrium constants in Cu-based atom transfer radical polymerization (ATRP) were determined for a wide range of ligands and initiators in acetonitrile at 22 °C. The ATRP equilibrium constants obtained vary over 7 orders of magnitude and strongly depend on the ligand and initiator structures. The activities of the Cu^{I}/ligand complexes are highest for tetradentate ligands, lower for tridentate ligands, and lowest for bidentate ligands. Complexes with tripodal and bridged ligands (Me_6TREN and bridged cyclam) tend to be more active than those with the corresponding linear ligands. The equilibrium constants are largest for tertiary alkyl halides and smallest for primary alkyl halides. The activities of alkyl bromides are several times larger than those of the analogous alkyl chlorides. The equilibrium constants are largest for the nitrile derivatives, followed by those for the benzyl derivatives and the corresponding esters. Other equilibrium constants that are not readily measurable were extrapolated from the values for the reference ligands and initiators. Excellent correlations of the equilibrium constants with the $Cu^{II/I}$ redox potentials and the carbon–halogen bond dissociation energies were observed.

Introduction

Atom transfer radical polymerization (ATRP, Scheme 1) is one of the most powerful and robust controlled radical polymerization (CRP) techniques.[1–5] The rate of ATRP depends on the value of the ATRP equilibrium constant (K_{ATRP}), i.e., the ratio of the rate constants for activation and deactivation (eq 1). The polydispersity (M_w/M_n) of the polymers obtained depends on the ratio of the propagation rate constant (k_p) to the deactivation rate constant (k_{deact}), the concentration of the deactivator $X-Cu^{II}Y/L_n$ (denoted as $[Cu^{II}]$), the concentration of the initiator ([RX]), monomer conversion (p), and the targeted degree of polymerization (DP_n) (eq 2). The activation rate constant (k_{act}) has been extensively examined in the literature.[2,6–23] Direct determination of k_{deact} is more difficult.[6,7,24,25] On the other hand, values of k_{deact} can be calculated from the equation $k_{deact} = k_{act}/K_{ATRP}$ if values of both k_{act} and K_{ATRP} are known. Therefore, determination of K_{ATRP} values is very important. The rate of polymerization of a given monomer (M) depends on the value of k_p and on the radical concentration ($[P_m^{\bullet}]$), which is determined by K_{ATRP} (eq 1). Thus, the evaluation of K_{ATRP} is

[†] Carnegie Mellon University.
[‡] Australian National University.

(1) Wang, J.-S.; Matyjaszewski, K. *J. Am. Chem. Soc.* **1995**, *117*, 5614–5615.
(2) Matyjaszewski, K. *J. Macromol. Sci., Pure Appl. Chem.* **1997**, *A34*, 1785–1801.
(3) Matyjaszewski, K.; Xia, J. *Chem. Rev.* **2001**, *101*, 2921–2990.
(4) Goto, A.; Fukuda, T. *Prog. Polym. Sci.* **2004**, *29*, 329–385.
(5) Matyjaszewski, K. *Prog. Polym. Sci.* **2005**, *30*, 858–875.
(6) Matyjaszewski, K.; Paik, H.-j.; Zhou, P.; Diamanti, S. J. *Macromolecules* **2001**, *34*, 5125–5131.
(7) Matyjaszewski, K.; Goebelt, B.; Paik, H.-j.; Horwitz, C. P. *Macromolecules* **2001**, *34*, 430–440.
(8) Matyjaszewski, K.; Paik, H.-j.; Shipp, D. A.; Isobe, Y.; Okamoto, Y. *Macromolecules* **2001**, *34*, 3127–3129.
(9) Matyjaszewski, K. *Macromolecules* **2002**, *35*, 6773–6781.
(10) Pintauer, T.; Zhou, P.; Matyjaszewski, K. *J. Am. Chem. Soc.* **2002**, *124*, 8196–8197.
(11) Nanda, A. K.; Matyjaszewski, K. *Macromolecules* **2003**, *36*, 599–604.
(12) Nanda, A. K.; Matyjaszewski, K. *Macromolecules* **2003**, *36*, 1487–1493.
(13) Nanda, A. K.; Matyjaszewski, K. *Macromolecules* **2003**, *36*, 8222–8224.
(14) Pintauer, T.; Braunecker, W.; Collange, E.; Poli, R.; Matyjaszewski, K. *Macromolecules* **2004**, *37*, 2679–2682.
(15) Matyjaszewski, K.; Nanda, A. K.; Tang, W. *Macromolecules* **2005**, *38*, 2015–2018.
(16) Tang, W.; Nanda, A. K.; Matyjaszewski, K. *Macromol. Chem. Phys.* **2005**, *206*, 1171–1177.
(17) Tang, W.; Matyjaszewski, K. *Macromolecules* **2006**, *39*, 4953–4959.
(18) Tang, W.; Matyjaszewski, K. *Macromolecules* **2007**, *40*, 1858–1863.
(19) Chambard, G.; Klumperman, B.; German, A. L. *Macromolecules* **2000**, *33*, 4417–4421.
(20) Goto, A.; Fukuda, T. *Macromol. Rapid Commun.* **1999**, *20*, 633–636.
(21) Ohno, K.; Goto, A.; Fukuda, T.; Xia, J.; Matyjaszewski, K. *Macromolecules* **1998**, *31*, 2699–2701.
(22) Schellekens, M. A. J.; de Wit, F.; Klumperman, B. *Macromolecules* **2001**, *34*, 7961–7966.
(23) Venkatesh, R.; Vergouwen, F.; Klumperman, B. *Macromol. Chem. Phys.* **2005**, *206*, 547–552.
(24) Chambard, G.; Klumperman, B.; German, A. L. *Macromolecules* **2002**, *35*, 3420–3425.
(25) Gromada, J.; Matyjaszewski, K. *Macromolecules* **2002**, *35*, 6167–6173.

10.1021/ja802290a CCC: $40.75

Scheme 1. Proposed Mechanism for Atom Transfer Radical Polymerization

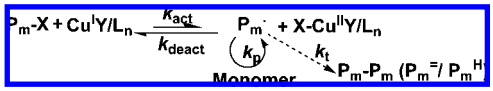

crucial for deeper understanding of this catalytic system and for optimal catalyst selection, especially for newly developed ATRP systems that use low concentrations of the catalyst $Cu^{I}Y/L_n$ (i.e., [Cu^{I}] on the order of ppm).[26,27] Small values of K_{ATRP} ($\sim 10^{-9}$ to $\sim 10^{-4}$) are required in order to maintain a low radical concentration and minimize termination reactions. The apparent K_{ATRP} ($K_{ATRP}^{app} = K_{ATRP}/[Cu^{II}]$) can be estimated from the kinetic plot of $\ln([M]_0/[M])$ versus time for an ATRP experiment;[28] however, precise values for K_{ATRP} are difficult to measure during polymerization because Cu^{II} concentrations continuously change as a result of the persistent radical effect (PRE), which is described in the Results and Discussion.[29]

$$\ln\left(\frac{[M]_0}{[M]_t}\right) = \frac{k_p K_{ATRP}[P_mX][Cu^I]}{[Cu^{II}]}t \quad (1)$$

$$\frac{M_w}{M_n} = 1 + \frac{1}{DP_n} + \left(\frac{k_p([RX]_0 - [RX])}{k_{deact}[Cu^{II}]}\right)\left(\frac{2}{p} - 1\right) \quad (2)$$

Our group recently modified Fischer's original equations for the PRE and successfully applied the new equations to determine K_{ATRP} values for various ATRP catalytic systems by monitoring the amount of accumulated deactivator as a function of time.[30,31] Fischer's original equations, which assume constant values of the catalyst and initiator concentrations, correctly describe the PRE up to only $\sim$10% conversion of Cu^{I} to Cu^{II}, and consequently, they can only be used in the determination of relatively small values of K_{ATRP}.[32] For greater conversion of Cu^{I} to Cu^{II} (>10%) and larger values of K_{ATRP} ($>10^{-7}$), modified equations that take into account the changes in catalyst and initiator concentrations should be used, as shown in eqs 3 and 4, in which $I_0 = [RX]_0$, $C_0 = [Cu^{I}]_0$, and $Y = [Cu^{II}]$.[30] Equation 3 applies when $C_0 \neq I_0$:

$$F(Y) = \left(\frac{I_0C_0}{C_0 - I_0}\right)^2\left[\frac{1}{C_0^2(I_0 - Y)} + \frac{2}{I_0C_0(C_0 - I_0)}\ln\left(\frac{I_0 - Y}{C_0 - Y}\right) + \frac{1}{I_0^2(C_0 - Y)}\right] = 2k_tK_{ATRP}^2t + c' \quad (3)$$

where k_t is the termination rate constant and c' is given by the expression

$$c' = \left(\frac{I_0C_0}{C_0 - I_0}\right)^2\left[\frac{1}{C_0^2I_0} + \frac{2}{I_0C_0(C_0 - I_0)}\ln\frac{I_0}{C_0} + \frac{1}{I_0^2C_0}\right]$$

Equation 4 must be used when $C_0 = I_0$:

$$F(Y) = \frac{C_0^2}{3(C_0 - Y)^3} + \frac{C_0}{(C_0 - Y)^2} + \frac{1}{C_0 - Y} = 2k_tK_{ATRP}^2t + \frac{1}{3C_0} \quad (4)$$

In either case, a plot of $F(Y)$ versus t should give a straight line, and the equilibrium constant for the reaction can be calculated from the slope (m) using the formula $K_{ATRP} = (m/2k_t)^{1/2}$. In our calculations, a k_t value of $= 2.5 \times 10^9$ M^{-1} s^{-1} (obtained for model small radicals in acetonitrile at 22 °C) was used.[33] UV−vis spectrometry and gas chromatography were used to follow the evolution of the Cu^{II} species and the initiator concentration, respectively, for several catalysts and alkyl halide initiators, from which the corresponding values of K_{ATRP} were determined.[30]

In this work, we present a large set of K_{ATRP} values determined for ATRP using various alkyl halide initiators and Cu catalysts with nitrogen-based ligands, and we discuss how the structures of the ligands and initiators affect the K_{ATRP} values. Values of K_{ATRP} that were not readily available were extrapolated by assuming similar selectivities of alkyl halides for various complexes.

Experimental Section

Materials. *N*-(*n*-Propyl)pyridylmethanimine (NPPMI) and *N*-(*n*-octyl)pyridylmethanimine (NOPMI) were synthesized by condensation of *n*-propylamine and *n*-octylamine, respectively, with pyridine-2-carboxaldehyde.[34] Tris(2-(dimethylamino)ethyl)amine (Me_6TREN) was synthesized by methylation of tris(2-aminoethyl)amine (TREN).[35] Tris(2-(diethylamino)ethyl)amine (Et_6TREN) was synthesized according to the literature.[36] Tris(2-(di-(2-cyanoethyl)amino)ethyl)amine (AN_6TREN), tris(2-(di-(2-(methoxycarbonyl)ethyl)amino)ethyl)amine (MA_6TREN), and tris(2-(di-(2-(*n*-butoxycarbonyl)ethyl)amino)ethyl)-amine (BA_6TREN) were synthesized by Michael addition of TREN to acrylonitrile, methyl acrylate, and *n*-butyl acrylate, respectively.[37] 2,5,9,12-Tetramethyl-2,5,9,12-tetraazatridecane (N4[2,3,2]),[38] 2,6,9,13-tetramethyl-2,6,9,13-tetraazatetradecane (N4[3,2,3]),[38] 4,11-dimethyl-1,4,8,11-tetraazabicyclo[6.6.2]hexadecane (Cyclam-B),[39,40] *N*′,*N*″-dimethyl-*N*′,*N*″-bis((pyridin-2-yl)methyl)ethane-1,2-diamine (BPED),[41] 4,4′-di-(5-nonyl)-2,2′-bipyridine (dNbpy),[42] and tris[(2-pyridyl)methyl]-amine (TPMA)[43] were synthesized according to the literature. 2,5,8,12-Tetramethyl-2,5,8,12-tetraazatridecane (N4[2,2,3]) was synthesized by a similar methylation of 2,5,8,12-tetraazatridecane tetrahydrochloride salt with formaldehyde and formic acid and distilled under reduced

(26) Matyjaszewski, K.; Jakubowski, W.; Min, K.; Tang, W.; Huang, J.; Braunecker, W. A.; Tsarevsky, N. V. *Proc. Natl. Acad. Sci. U.S.A.* **2006**, *103*, 15309–15314.
(27) Jakubowski, W.; Matyjaszewski, K. *Angew. Chem., Int. Ed.* **2006**, *45*, 4482–4486.
(28) Qiu, J.; Matyjaszewski, K.; Thouin, L.; Amatore, C. *Macromol. Chem. Phys.* **2000**, *201*, 1625–1631.
(29) Fischer, H. *Chem. Rev.* **2001**, *101*, 3581–3610.
(30) Tang, W.; Tsarevsky, N. V.; Matyjaszewski, K. *J. Am. Chem. Soc.* **2006**, *128*, 1598–1604.
(31) Tang, W.; Fukuda, T.; Matyjaszewski, K. *Macromolecules* **2006**, *39*, 4332–4337.
(32) Fischer, H. *J. Polym. Sci., Part A: Polym. Chem.* **1999**, *37*, 1885–1901.
(33) Fischer, H.; Radom, L. *Angew. Chem., Int. Ed.* **2001**, *40*, 1340–1371.
(34) Haddleton, D. M.; Clark, A. J.; Crossman, M. C.; Duncalf, D. J.; Heming, A. M.; Morsley, S. R.; Shooter, A. J. *Chem. Commun* **1997**, 1173.
(35) Queffelec, J.; Gaynor, S. G.; Matyjaszewski, K. *Macromolecules* **2000**, *33*, 8629–8639.
(36) Inoue, Y.; Matyjaszewski, K. *Macromolecules* **2004**, *37*, 4014–4021.
(37) Zeng, F.; Shen, Y.; Zhu, S.; Pelton, R. *Macromolecules* **2000**, *33*, 1628–1635.
(38) Golub, G.; Cohen, H.; Paoletti, P.; Bencini, A.; Messori, L.; Bertini, I.; Meyerstein, D. *J. Am. Chem. Soc.* **1995**, *117*, 8353–8361.
(39) Wong, E. H.; Weisman, G. R.; Hill, D. C.; Reed, D. P.; Rogers, M. E.; Condon, J. S.; Fagan, M. A.; Calabrese, J. C.; Lam, K.-C.; Guzei, I. A.; Rheingold, A. L. *J. Am. Chem. Soc.* **2000**, *122*, 10561–10572.
(40) Tsarevsky, N. V.; Braunecker, W. A.; Tang, W.; Brooks, S. J.; Matyjaszewski, K.; Weisman, G. R.; Wong, E. H. *J. Mol. Catal. A: Chem.* **2006**, *257*, 132–140.
(41) Xia, J.; Zhang, X.; Matyjaszewski, K. *ACS Symp. Ser.* **2000**, *760*, 207–223.
(42) Matyjaszewski, K.; Patten, T. E.; Xia, J. *J. Am. Chem. Soc.* **1997**, *119*, 674–680.
(43) Xia, J.; Matyjaszewski, K. *Macromolecules* **1999**, *32*, 2434–2437.

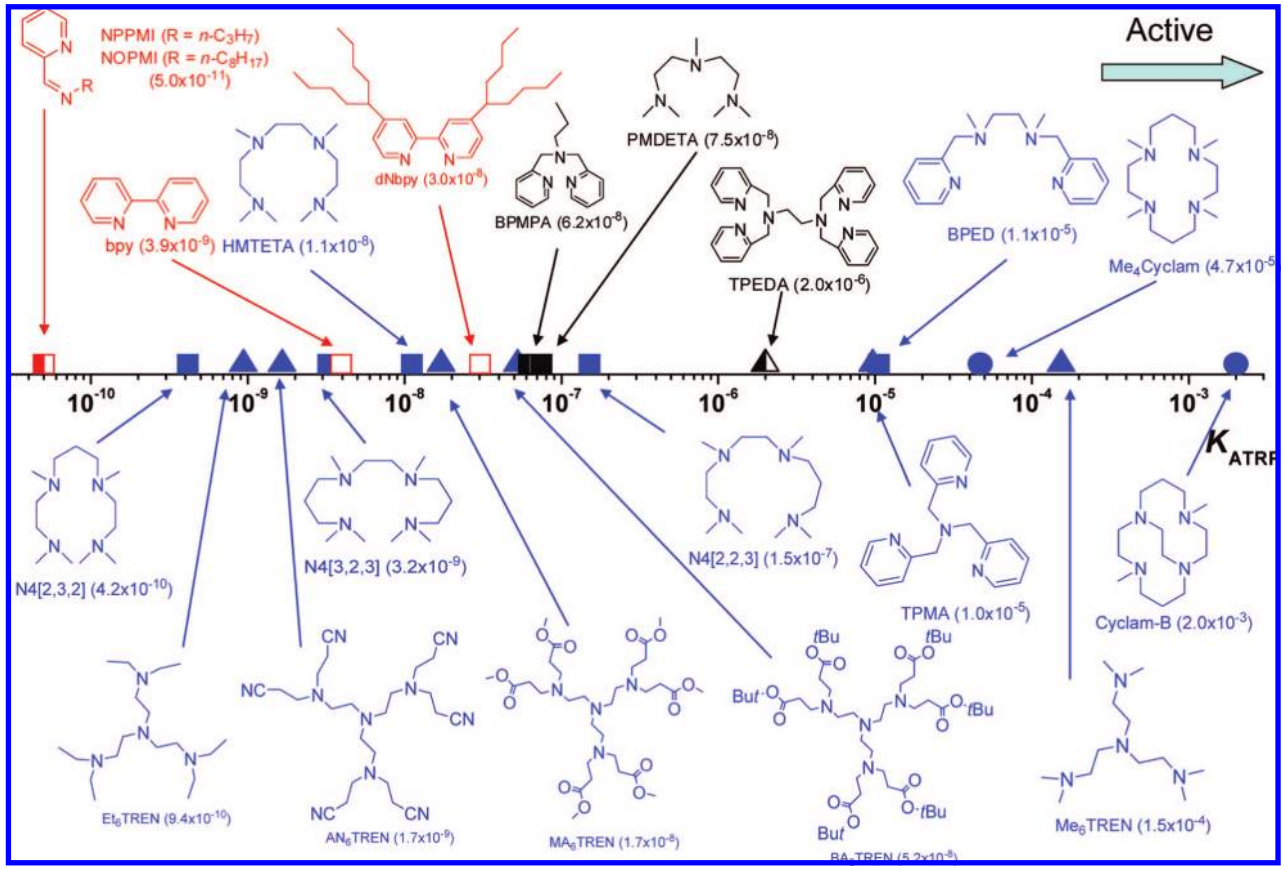

Figure 1. ATRP equilibrium constants K_{ATRP} for various N-based ligands with the initiator EtBriB in the presence of $Cu^{I}Br$ in MeCN at 22 °C. Color key: (red) N2; (black) N3 and N6; (blue) N4. Symbol key: (solid) amine/imine; (open) pyridine; (left-half-solid) mixed; (□) linear; (△) branched; (○) cyclic.

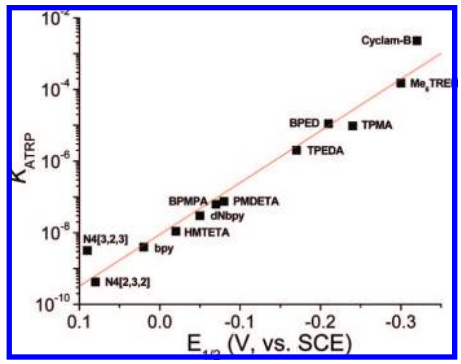

Figure 2. Plot of K_{ATRP} (measured with EtBriB) vs $E_{1/2}$ for 12 $Cu^{II}Br_2$/L complexes.

pressure. *N*,*N*,*N*′,*N*′-Tetra[(2-pyridyl)methyl]ethylenediamine (TPEDA) was synthesized by a reaction of benzyl chloride and ethylenediamine.[44] *N*-[2-(Dimethylamino)ethyl]-*N*,*N*′,*N*′-trimethyl-1,3-propanediamine (N3[2,3]) was synthesized by methylation of *N*-(2-aminoethyl)-1,3-propanediamine. All of the other ligands, initiators, and solvents were used as received. Abbreviations for the ligands[17] and initiators[18] are listed in Figures 1 and 3.

Determination of Equilibrium Constants. Typical procedures for determination of the equilibrium constants can be found in our previous report.[30] The K_{ATRP} values for exceptionally fast or slow systems were estimated from those for slower or faster systems, respectively. For example, K_{ATRP} for $Cu^{I}Br$/Cyclam-B with EtBriB was estimated from the value for $Cu^{I}Cl$/Cyclam-B with MClAc as follows: $K_{ATRP}(Cu^{I}Br/\text{Cyclam-B with EtBriB}) = K_{ATRP}(Cu^{I}Cl/\text{Cyclam-B with MClAc}) \times K_{ATRP}(Cu^{I}Br/\text{TPMA with EtBriB})/K_{ATRP}(Cu^{I}Cl/\text{TPMA with MClAc}) = (9.9 \times 10^{-5})(9.6 \times 10^{-6})/(4.2 \times 10^{-7}) = 2.3 \times 10^{-3}$.

Cyclic Voltammetry. All of the voltammograms were recorded at 25 °C with a Gamry Reference 600 potentiostat. Solutions of $Cu^{II}Br_2$/L (1.0 mM) were prepared in dry solvent containing 0.1 M Bu_4NPF_6 as the supporting electrolyte. Measurements were carried out under nitrogen at a scan rate of 0.1 V s^{-1} using a glassy carbon disk as the working electrode and a platinum wire as the counter electrode. Potentials were recorded versus SCE using a 0.1 M Bu_4NPF_6 salt bridge to minimize contamination of the analyte with Cl^{-} ions.

Calculation of Bond Dissociation Energies. R−X bond dissociation energies (BDEs) for the alkyl halides in acetonitrile at 22 °C were taken directly from a recent study.[45] The data in this study were obtained via standard ab initio molecular orbital theory calculations performed at a high level of theory chosen on the basis of recent assessment studies for alkyl halide homolytic BDEs.[46,47] Geometries and frequencies were obtained at the B3LYP/6-31+G(d) level of theory, and improved energies were obtained using the high-level composite method G3(MP2)-RAD(+). Partition functions and associated thermodynamic functions (i.e., entropies and temperature corrections) were evaluated using the TES 60 °C hindered-

(44) Tang, H.; Arulsamy, N.; Radosz, M.; Shen, Y.; Tsarevsky, N. V.; Braunecker, W. A.; Tang, W.; Matyjaszewski, K. *J. Am. Chem. Soc.* **2006**, *128*, 16277–16285.

(45) Lin, C. Y.; Coote, M. L.; Gennaro, A.; Matyjaszewski, K. *J. Am. Chem. Soc.*, submitted for publication, 2008.

(46) Izgorodina, E. I.; Coote, M. L.; Radom, L. *J. Phys. Chem. A* **2005**, *109*, 7558–7566.

(47) Izgorodina, E. I.; Brittain, D. R. B.; Hodgson, J. L.; Krenske, E. H.; Lin, C. Y.; Namazian, M.; Coote, M. L. *J. Phys. Chem. A* **2007**, *111*, 10754–10768.

rotor model,[48] and free energies of solvation were evaluated using the CPCM continuum model at the HF/6-31+G(d) level of theory in conjunction with UAHF radii. All of the calculations were performed using Gaussian 03.[49]

Results and Discussion

Effect of Ligand Structure on Equilibrium Constants. To compare the activities of Cu^{I} complexes containing various nitrogen-based ligands, most of the experiments were carried out under the same conditions, i.e., in the same solvent (acetonitrile), at the same temperature (22 °C), and with the same initiator (EtBriB). Figure 1 shows the measured K_{ATRP} values on a logarithmic scale. The activities of the catalysts formed with these ligands range over 7 orders of magnitude.

It was previously reported that the catalysts become more active when the Cu^{II} state of the catalyst is better stabilized by the ligand.[7,41,50] In general, the activities of complexes with various ligands decrease in the following order: alkyl amine ≈ pyridine > alkyl imine ≫ aryl imine > aryl amine. They also decrease as the number of nitrogens in the ligand decreases.[7,41] The present results generally confirm such observations, but some other factors, including steric and electronic effects and bite angle, are also important and are discussed in the next section.[51,52]

Correlation of Catalyst Structure with ATRP Activity and Electrochemistry. As the ATRP equilibrium is governed by a redox process between the higher and lower oxidation states of a transition-metal catalyst, electrochemistry can be a useful tool for understanding and predicting catalytic activity.[50,53] The general trend that more reducing complexes are better catalysts (i.e., yield greater rates of polymerization) has been observed among complexes of the same metal for a wide range of Cu,[6,28,30,40,54] Fe,[55,56] and Ru-based catalysts.[57] In fact, a linear correlation between the logarithm of K_{ATRP}^{app} (determined from rates of catalyzed polymerization) and measured $E_{1/2}$ values for Cu complexes of Me_6TREN, TPMA, PMDETA, and derivatives of bpy and BPMODA (complexes also used in this study) has been observed.[28] However, exceptionally active catalysts can generate a large number of radicals at the early stages of polymerization that terminate before the system reaches equilibrium. Since these termination reactions result in the irreversible accumulation of the ATRP deactivator (a phenomenon termed the *persistent radical effect*), it is possible that more active ATRP catalysts actually give rise to slower polymerizations and/or reactions that stop after relatively low monomer conversion.[30] The K_{ATRP} value, as quantified via model reactions, is therefore a more accurate measure of catalyst activity than the rate of catalyzed polymerization.

Table 1. CV Data for $Cu^{II}Br_2$/L Complexes in Acetonitrile[a]

ligand	$E_{p,a}$ (V)[b]	$E_{p,c}$ (V)[c]	ΔE_p (mV)	i_b/i_f[d]	$E_{1/2}$ (V)[e]
Cyclam	−0.890	−1.000	110	0.87	−0.95
Me_4Cyclam	−	−0.446	−	<0.01	−
Cyclam-B	−0.270	−0.361	91	0.89	−0.32
Me_6TREN	−0.258	−0.339	81	0.89	−0.30
TPMA	−0.206	−0.276	70	0.95	−0.24
BPED	−0.160	−0.264	104	0.94	−0.21
TPEDA	−0.137	−0.210	73	0.90	−0.17
PMDETA	−0.026	−0.128	102	0.90	−0.08
BPMPA	−0.012	−0.119	107	0.92	−0.07
dNbpy	−0.006	−0.095	89	0.99	−0.05
HMTETA	0.058	−0.097	155	0.84	−0.02
N4[2,2,3]	0.083	−0.065	148	0.67	0.01
bpy	0.084	−0.037	121	0.97	0.02
N4[2,3,2]	0.191	−0.041	232	0.76	0.08
N4[3,2,3]	0.129	0.041	88	0.91	0.09
ferrocene	0.458	0.388	70	1.00	0.42

[a] Conditions: 0.1 M NBu_4PF_6, 1.0 mM $Cu^{II}Br_2$/L complex, scan rate 0.10 V s^{-1}. Potentials are reported vs SCE. [b] Peak potential of the oxidation wave. [c] Peak potential of the reduction wave. [d] backward-to-forward peak current ratio. [e] $E_{1/2} = (E_{p,a} + E_{p,c})/2$.

Table 1 summarizes cyclic voltammetry (CV) data recorded for 15 ATRP catalysts in acetonitrile. The majority of the complexes investigated showed good (quasi)reversibility under these conditions, as judged by their relatively small ΔE_p values and their backward-to-forward peak current ratios (i_b/i_f), which had values close to unity. Figure 2 shows the correlation of the logarithmic values of K_{ATRP} with measured $E_{1/2}$ values from the more-reversible voltammograms of 12 catalysts (those for which $i_b/i_f > 0.75$).

The excellent correlation between ATRP activities and values of $E_{1/2}$ for a wide range of complexes, as observed in Figure 2, warrants an in-depth discussion of how various ligand morphologies and substituents affect the $Cu^{II/I}$ redox potentials and thereby govern catalyst activities. While parametrization methods have been successfully employed to predict redox potentials among complexes having the same metal, stereochemistry, and oxidation and spin states,[58] such parametrization techniques are inadequate for predicting the activity of most Cu-containing ATRP catalysts because the application of multidentate ligands introduces varying degrees of distortion from ideal or preferred geometries. Nevertheless, some general rules still apply.[50] For example, the introduction of electron-withdrawing groups on the ligand results in less-reducing complexes while electron-donating groups increase the reducing power of a complex. Specific examples and ligand morphologies illustrated in Figure 2 are discussed in the following paragraphs.

Linear Tetradentate Ligands. Four linear aliphatic tetradentate ligands having various ethylene and propylene linking units were studied. N4[2,2,2] and N4[2,2,3] form relatively active catalysts having K_{ATRP} values of 1.1×10^{-8} and 1.5×10^{-7}, respectively, but N4[2,3,2] and N4[3,2,3] form less-active catalysts having K_{ATRP} values of 4.2×10^{-10} and 3.2×10^{-9}, respectively. The order of reducing power measured in acetonitrile is consistent with literature values recorded in water, i.e., the Cu complex with N4[2,2,2] (HMTETA) is more reducing (and more active) than the complex with N4[2,3,2], which is slightly more reducing than the one with N4[3,2,3].[38] While these ligands all have essentially the same basicity and electronic properties, their redox potentials vary by

(48) Lin, C. Y.; Izgorodina, E. I.; Coote, M. L. *J. Phys. Chem. A* **2008**, *112*, 1956–1964.
(49) Frisch, M. J.; et al. *Gaussian 03*, revision B.03; Gaussian, Inc.: Wallingford, CT, 2003.
(50) Tsarevsky, N. V.; Matyjaszewski, K. *Chem. Rev.* **2007**, *107*, 2270–2299.
(51) Levy, A. T.; Patten, T. E. *Polym. Mater. Sci. Eng.* **1999**, *80*, 467–468.
(52) Pintauer, T.; Matyjaszewski, K. *Coord. Chem. Rev.* **2005**, *249*, 1155–1184.
(53) Tsarevsky, N. V.; Tang, W.; Brooks, S. J.; Matyjaszewski, K. *ACS Symp. Ser.* **2006**, *944*, 56.
(54) Tsarevsky, N. V.; Braunecker, W. A.; Brooks, S. J.; Matyjaszewski, K. *Macromolecules* **2006**, *39*, 6817–6824.
(55) O'Reilly, R. K.; Gibson, V. C.; White, A. J. P.; Williams, D. J. *J. Am. Chem. Soc.* **2003**, *125*, 8450–8451.
(56) O'Reilly, R. K.; Gibson, V. C.; White, A. J. P.; Williams, D. J. *Polyhedron* **2004**, *23*, 2921–2928.
(57) Ando, T.; Kamigaito, M.; Sawamoto, M. *Macromolecules* **2000**, *33*, 5825–5829.
(58) Lever, A. B. P. *Inorg. Chem.* **1990**, *29*, 1271–1285.

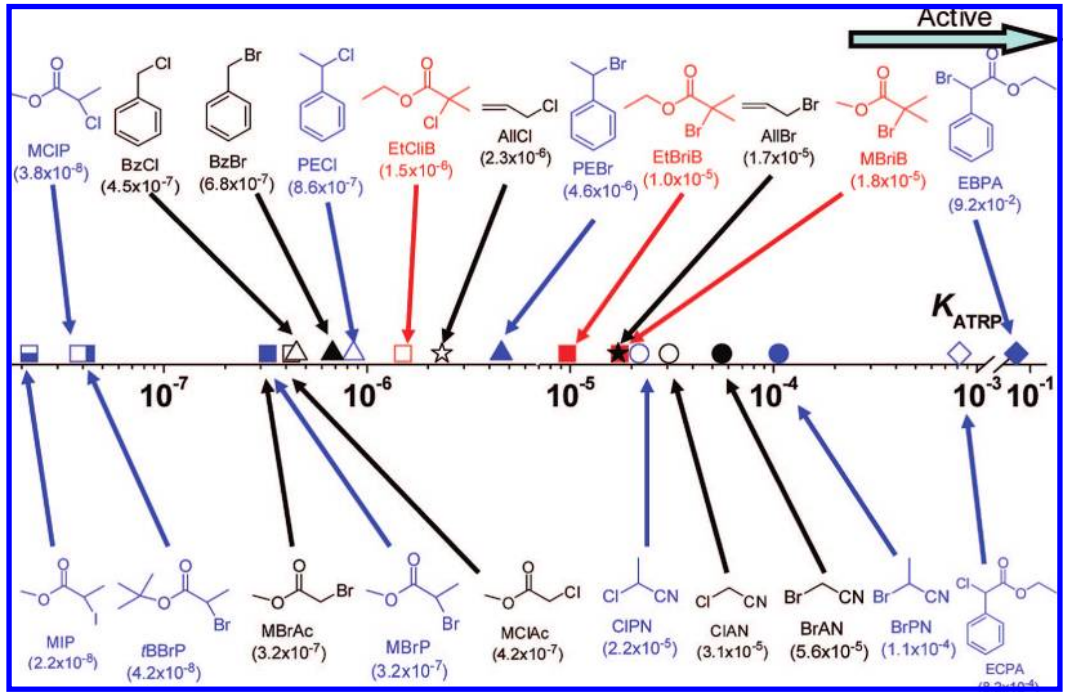

Figure 3. ATRP equilibrium constants for various initiators with $Cu^{I}X$/TPMA (X = Br, Cl) in MeCN at 22 °C. Color key: (red) 3°; (blue) 2°; (black) 1°. Symbol key: (solid) R−Br; (open) R−Cl; (bottom-half-solid) R−I; (△) phenyl; (□) ester; (○) nitrile; (◇) phenyl ester; (☆) allyl.

110 mV. The main difference between these ligands is the relative location of the propylene linker, which increases the preferred chelating angle from 70 to 109° and, by inducing additional reducing strength, decreases the stability of the Cu^{II} complex that determines K_{ATRP}. This shows how subtle differences in catalyst structure can have dramatic effects on the relative stabilities of the Cu^{I} and Cu^{II} oxidation states.

Replacing the two aliphatic amines on the ends of HMTETA with aromatic pyridyl groups (to form BPED) results in a ligand whose copper bromide complex is 190 mV more reducing and precisely 3 orders of magnitude more active in ATRP ($K_{ATRP} = 1.1 \times 10^{-5}$ for BPED). The relative reducing power of the BPED complex is surprising, given that substituting aliphatic nitrogens with aromatic ones typically results in Cu^{I} compounds that are much less reducing.[59] However, this anomaly can be partially rationalized when the structure of the analogous nonmethylated Cu^{II}/BPED complex discussed in the literature is considered. Spectroscopic evidence indicates that the Cu^{II} structure is quite planar and more rigid than those of some analogous compounds. This effectively results in a relative increase in the stability of the Cu^{II} oxidation state over the Cu^{I} state, as the latter is less able to accommodate a planar structure, preferring instead a tetrahedral geometry.[60]

Tripodal/Branched Tetradentate Ligands. Cu complexes with Me_6TREN form some of the most active ($K_{ATRP} = 1.5 \times 10^{-4}$) and most reducing catalysts successfully employed in ATRP. They were also successfully used in the new ATRP systems that employ only parts per million levels of Cu catalyst.[26] In a manner that is qualitatively consistent with literature predictions,[59] replacing the aliphatic amine nitrogens of ME_6TREN with aromatic ones (to form TPMA) results in a Cu complex that is slightly less reducing and less active ($K_{ATRP} = 1.0 \times 10^{-5}$). Furthermore, it has been observed that by progressively increasing the electron-donating power of the para substituents on the pyridyl rings of TPMA (through the use of *p*-H-, *p*-*t*-Bu-, *p*-MeO-, and *p*-Me_2N-substituted ligands), one can increase the reducing power of the Cu complexes by 300 mV (corresponding to an increase of 5 orders of magnitude in the equilibrium constant for electron transfer).[61] In a similar fashion, the electron-withdrawing power of TREN-based ligands was progressively increased in the present study by using −Me, $-(CH_2)_2CO_2t$Bu, $-(CH_2)_2CO_2$Me, and $-(CH_2)_2$CN substituents on the ethylamine nitrogens. As expected, the values of K_{ATRP} for these ligands decreased (spanning 5 orders of magnitude) as the electron-withdrawing power of the ligand and steric effects increased.

Macrocyclic Ligands. The stability constants for Cu^{II} complexes of macrocyclic ligands such as Cyclam and its derivatives are quite large ($\sim 10^{27}$ in water).[62] In addition, these relatively rigid ligands form planar complexes that do not stabilize the tetrahedral Cu^{I} oxidation state very well. As a consequence of these two facts, Cu^{I} complexes with Cyclam-type ligands tend to form exceptionally reducing and active catalysts in ATRP.

Ideally, the effect on catalyst activity of substituting −H with −Me among complexes of Cyclam and Me_4Cyclam could be studied. Unfortunately, because Cu^{I}Br/Cyclam is so exceptionally reducing, the complex was far too active to accurately determine K_{ATRP}, even when alkyl halide initiators with low activities were used. Furthermore, the voltammogram for the complex with Me_4Cyclam was not reversible, making a direct comparison of the redox potentials of the two complexes impossible. The activities and reducing power of the catalysts could still be compared, however, by employing the trend line

(59) Addison, A. W. *Inorg. Chim. Acta* **1989**, *162*, 217–220.
(60) Zanello, P. In *Stereochemical Control, Bonding and Steric Rearrangements*; Bernal, I., Ed.; Elsevier: Amsterdam, 1990; Vol. 4, pp 181−366.
(61) Zhang, C. X.; Kaderli, S.; Costas, M.; Kim, E.-i.; Neuhold, Y.-M.; Karlin, K. D.; Zuberbühler, A. D. *Inorg. Chem.* **2003**, *42*, 1807–1824.
(62) Sun, X.; Wuest, M.; Weisman, G. R.; Wong, E. H.; Reed, D. P.; Boswell, C. A.; Motekaitis, R.; Martell, A. E.; Welch, M. J.; Anderson, C. J. *J. Med. Chem.* **2002**, *45*, 469–477.

generated from the data in Figure 2. In this manner, one can see that Cyclam complex ($E_{1/2} \approx -0.95$ V vs SCE) should be >10 orders of magnitude more active than the complex with Me_4Cyclam ($K_{ATRP} = 4.7 \times 10^{-5}$), consistent with the trend observed in the literature that substituting −H with −Me yields complexes that are significantly less reducing. This has been seen not only for macrocyclic ligands but also for linear and branched aliphatic amines. This observation contradicts the "rule" that increasing the electron-donating power of a substituent results in a more-reducing complex and cannot be attributed merely to a distortion of preferred geometries, as analogous results have been observed for a wide variety of metals preferring a wide variety of geometries. It was, however, concluded that N-alkylation effectively induces a strain on the ligand skeleton that is naturally smaller for the Cu^I complexes than for the Cu^{II} complexes, i.e., N-alkylation of ligands increases their binding constants for large cations but decreases their binding constants for small cations.[38]

Cyclam-B has a special bridged cyclic structure in which an ethylene group cross-bridges two diagonal nitrogens. The Cu^I/Cyclam-B catalyst is by far the most active ATRP catalyst: it can successfully mediate ATRP with a K_{ATRP} value ~13 times larger than that of Me_6TREN.[40] The ligand TPEDA was the only hexadentate ligand studied here. The Cu^IBr complex formed by this ligand is fairly active (25 times more active than Cu^IBr/PMDETA but ~75 times less active than Cu^IBr/Me_6TREN).[44]

Bi- and Tridentate Ligands. Cu^IBr complexes with two bidentate pyridine imine ligands are some of the least active ATRP catalysts ($K_{ATRP} = 5.0 \times 10^{-11}$ for both NPPMI and NOPMI). This observation is consistent with the positive redox potentials reported in the literature for structurally related complexes.[60] Catalysts employing bipyridine ligands, the first developed for Cu-based ATRP, are more active than the pyridine imines ($K_{ATRP} = 3.9 \times 10^{-9}$ for bpy). Long alkyl groups were incorporated onto the pyridine rings in order to increase the solubility of the catalyst in less polar solvents. However, these alkyl substituents also increased the catalytic activity by an order of magnitude ($K_{ATRP} = 3.0 \times 10^{-8}$ for dNbpy), as the electron-donating groups made the catalyst more reducing.

Cu^IBr complexes with two different tridentate ligands, PMDETA and BPMPA, were also investigated. Cu^IBr/PMDETA ($K_{ATRP} = 7.5 \times 10^{-8}$) was slightly more active and more reducing than the BPMPA complex bearing two pyridylmethyl groups. However, it should be noted that the complexes of these ligands with Cu^IX are atypical of traditional Cu^I-based catalysts in that the halide anion also acts as a ligand rather than just a counterion. Under polymerization conditions, where a substantial amount of vinyl monomer coordinates to Cu^I/PMDETA by displacing the halide ligand,[63] the redox potentials and hence the values of K_{ATRP} may not accurately reflect the true polymerization activity of the catalyst. When the two amino groups in PMDETA were replaced with pyridyl groups, the resulting BPMPA catalyst had a K_{ATRP} value of 6.2×10^{-8}, similar to that for PMDETA.

Effect of Initiator Structure on Equilibrium Constants. Similar methodology was employed to investigate the effect of initiator structure on K_{ATRP} in ATRP. Most of the bromine- and chlorine-based initiators as well as the iodine-based initiators for Cu-based ATRP were studied with the same catalyst, Cu^IX/TPMA. Using Cu^IX/TPMA as the catalyst afforded a fairly fast reaction for most of the initiators. As shown in Figure 3, the activity ratio among these initiators exceeds 10^5. The ATRP equilibrium constant K_{ATRP} can be defined as the product of the equilibrium constant for homolytic bond dissociation of R−X and that for formation of Cu^{II}−X from Cu^I and $X^\bullet$ (i.e., the halogenophilicity) (see Scheme 2). Thus, K_{ATRP} values should be correlated with the BDEs of the initiators. Unfortunately, there are very few experimental data available on BDEs of relevant alkyl halides, and the data exhibit significant scatter.[64] Therefore, we will first discuss the phenomenological dependence of the K_{ATRP} values on the most important structural parameters. Subsequently, we will compare the computationally accessible free energies of C−X bond dissociation with those estimated from K_{ATRP} measurements assuming constant halogenophilicity values for various alkyl halides.

Scheme 2. Atom-Transfer Equilibrium Represented as a Combination of Alkyl Halide Bond Homolysis and Cu^{II}−X Bond Formation (Halogenophilicity)

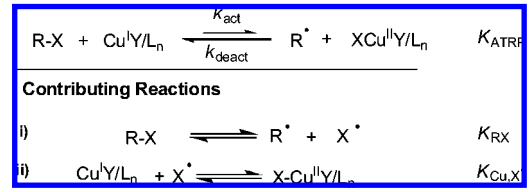

Effect of the Leaving Atom. Alkyl bromides are several times more active than the corresponding alkyl chlorides: for example, EtBriB (6) > EtCliB (1), BrPN (5) > ClPN (1), PEBr (5) > PECl (1), and MBrP (8) > MClP (1), where the numbers in parentheses are the relative K_{ATRP} values. The difference in the K_{ATRP} values for EtBriB and EtCliB facilitates the halogen-exchange technique required to synthesize well-defined (meth)acrylic block copolymers.[65] Although k_{act} for MIP is close to that for MBrP, K_{ATRP} for MIP is ~15 times smaller than that for MBrP. This is a consequence of the very low stability of the Cu^{II}−I bond.

Tertiary, Secondary, And Primary Alkyl Halides. The k_{act} values for tertiary, secondary, and primary ester initiators follow the order 3° > 2° > 1°.[18] The order of the K_{ATRP} values is similar, but there are some differences. Values of K_{ATRP} are ~30 times larger for tertiary haloisobutyrate esters than for secondary halopropionates. However, the difference between the values for secondary and primary species is smaller. For example, K_{ATRP} for BrPN is ~2 times larger than that for BrAN, and the same behavior is observed for MBrP and MBrAc as well as for PECl and BzCl. The difference for benzyl bromides is larger, however. It is possible that values of K_{ATRP} for alkyl halides that form very electrophilic primary radicals can be overestimated. The evolution of Cu^{II} species may be due not only to radical coupling (which is directly correlated with K_{ATRP}) but also to reduction of the radicals to carbanions by Cu^I species via an outer-sphere electron transfer (OSET) process.

Stabilization of Radicals by Substituents. Within a given initiator type, initiators with a nitrile substituent attached to the carbon atom of the C−X bond are more active than those with phenyl groups, which are in turn more active than initiators with

(63) Braunecker, W. A.; Tsarevsky, N. V.; Pintauer, T.; Gil, R. R.; Matyjaszewski, K. *Macromolecules* **2005**, *38*, 4081–4088.

(64) Gillies, M. B.; Matyjaszewski, K.; Norrby, P.-O.; Pintauer, T.; Poli, R.; Richard, P. *Macromolecules* **2003**, *36*, 8551–8559.

(65) Matyjaszewski, K.; Shipp, D. A.; McMurtry, G. P.; Gaynor, S. G.; Pakula, T. *J. Polym. Sci., Part A: Polym. Chem.* **2000**, *38*, 2023–2031.

ester groups. The orders of the K_{ATRP} values with Cu^IBr/TPMA for two types of bromide initiators were BrPN (340) > PEBr (14) > MBrP (1) and BrAN (175) ≫ BzBr (2) ≥ MBrAc (1). A similar order was also found for the chlorides. The differences in the equilibrium constants can be explained in terms of the competing effects of the substituents on the stability of the alkyl halide bond, which increases with the electron-donating ability of the substituent (i.e., cyano < ester < phenyl), and their effects on the stabilities of the alkyl radical formed (ester < cyano < phenyl).[66,67]

MBriB and EtBriB have similar values of K_{ATRP}, while *t*BBrP is ~8 times less active than MBrP. This could be attributed to the fact that the *tert*-butyl group is more bulky than a methyl group and introduces more steric congestion to the sp^2 hybridized radical than to the alkyl bromide.

The most active initiator is EBPA (a mixed benzyl−ester initiator), which is ~20,000 times more active than PEBr and 300,000 times more active than MBrP. This is due to the synergistic stabilization effect of the phenyl and carboxyethyl groups. EBPA is an efficient initiator for monomers with large equilibrium constants, such as acrylonitrile and methyl methacrylate.[26,27]

As illustrated in Figure 3, the ratio of the highest and lowest equilibrium constants for the alkyl halides in this study exceeds 10^5. These values were mostly measured by using Cu^IBr/TPMA as the catalyst in MeCN at 22 °C. The equilibrium constants increase with (a) initiator substitution [1° (black) < 2° (blue) < 3° (red)] and (b) the presence of radical-stabilizing groups for secondary initiators [−COOR (squares) < −Ph (triangles) ≪ −CN (circles) ≪ both −Ph and α-COOEt groups (diamonds)]; K_{ATRP} also depends on (c) the leaving atom/group [e.g., for methyl 2-halopropionates, iodide (bottom-half-solid) < chloride (open) < bromide (filled)].

Bond Dissociation Energies and Values of K_{ATRP}. As discussed above, experimental data on BDEs for alkyl halides relevant to ATRP are limited. However, both enthalpies and free energies of bond dissociation can be accessed computationally using density functional theory (DFT)[64] or ab initio[45] procedures. BDEs should correlate well with values of K_{ATRP}, since the ATRP equilibrium can be represented formally as a combination of two hypothetical reactions: (i) homolytic cleavage of the C−X bond in the alkyl halide and (ii) formation of the $X-Cu^{II}$ bond in the deactivator via the reaction of Cu^I with the halogen atom.[45]

As shown in Scheme 2, the first process is characterized by the equilibrium constant K_{RX}, which is related to the free energy of C−X bond dissociation (ΔG), which can be accessed computationally not only in vacuum but also in a solvent. Computed ΔG values and the corresponding values of log K_{RX} for alkyl halides at 295.15 K (22 °C) in MeCN are listed in Table 2. These values were obtained from the high-level ab initio calculations described in a related study.[45] The second process is characterized by the equilibrium constant $K_{Cu,X\cdot}$, which is called the halogenophilicity and indicates the affinity of the transition metal in its lower oxidation state for the halogen atom. Unfortunately, the value of $K_{Cu,X\cdot}$, which is the reciprocal of the equilibrium constant for homolytic bond dissociation of the $X-Cu^{II}$ species, cannot be directly measured, and its computation is complicated since the process involves reorganization of the transition-metal complex, including an expansion of the coordination sphere, a change in the oxidation state, and any related changes in its solvation state (including any specific solvation as well). On the other hand, $K_{Cu,X\cdot}$ can be calculated from K_{ATRP} and K_{RX} via the expression $K_{Cu,X\cdot} = K_{ATRP}/K_{RX}$. It should be noted that the value of $K_{Cu,X\cdot}$ depends on the type of ligand (L in Cu^IY/L) and the type of halogen (X).

Values of $K_{Cu,X\cdot}$ were calculated as the ratio K_{ATRP}/K_{RX} for each catalyst using EtBriB and EtCliB as reference compounds, since both haloisobutyrates were used in reactions with most catalysts. The resulting values of $K_{Cu,X\cdot}$ are listed in Table 2. These values are very large and are comparable to the reciprocal values of K_{RX}, since their product gives a much smaller value of K_{ATRP}. The halogenophilicities are larger for more-active catalysts and larger for chlorine than for bromine. Values of log $K_{Cu,Br\cdot}$ range from 27.1 (NPPMI) to 33.6 (Me_6TREN) and values of log $K_{Cu,Cl\cdot}$ from 38.5 (bpy) to 43.1 (Me_6TREN). Once the values of the halogenophilicities for various catalysts are known, they can be used together with values of K_{ATRP} to calculate bond-dissociation equilibrium constants ($K_{RX} = K_{ATRP}/K_{Cu,X\cdot}$). These values can then be compared with the ab initio computed values of K_{RX}. It should be noted that while the resulting experimental values of K_{RX} for the alkyl chlorides and alkyl bromides are, by necessity, effectively scaled by the respective ab initio values for EtCliB and EtBriB, their relative values are completely independent of the theoretical calculations. Hence, we can use the experimental K_{RX} values to assess the ability of the theoretical data to model the wide variation in K_{RX} and hence in K_{ATRP}.

Figure 4 presents a plot of log K_{ATRP} − log $K_{Cu,X\cdot}$ versus log K_{RX}, in which the green dashed line is the line with slope 1 that passes through the values for the two standards EtBriB and EtCliB. In general, there is an excellent correlation between the equilibrium constants obtained via the calculated BDEs and those obtained experimentally. In most cases, the scatter is within or close to the expected order-of-magnitude uncertainty in the theoretical calculations; however, there are some outliers. In particular, points above the line represent experimental values of K_{ATRP} that are larger than expected, plausibly as a result of the concurrent reduction of radicals to carbanions via OSET (e.g., entries 10 and 16 for MBrAc and 25 and 30 for MClAc). It should also be noted that Figure 4 was constructed assuming constant selectivities of initiators and catalysts, as will be discussed in the next section.

Overview of Different Structural Parameters Affecting the Equilibrium Constants. The structural effects of ligand and initiator on K_{ATRP} reported herein correlate very well with previously reported trends for k_{act}.[17,18] Most values of K_{ATRP} were obtained using EtBriB as a standard initiator for screening different catalysts and TPMA as a standard ligand for screening various alkyl halides. It is tempting to predict values of K_{ATRP} for other systems by assuming constant selectivities of alkyl halides toward various ligands and also constant selectivities of catalysts toward various initiators. In this way, one can extrapolate (or interpolate) the K_{ATRP} values to ligands with initiators other than EtBriB and initiators with ligands other than TPMA. The same strategy was previously employed for extrapolating k_{act} values for various catalysts and initiators.[18] The constant selectivity principle, i.e., the assumption that Cu^IBr/ligand has the same selectivity as Cu^IBr/TPMA toward more-active and less-active initiators, was verified for several systems, as shown in Table 3.

(66) Coote, M. L.; Henry, D. J. *Macromolecules* **2005**, *38*, 1415–1433.
(67) Krenske, E. H.; Izgorodina, E. I.; Coote, M. L. *ACS Symp. Ser.* **2006**, *944*, 406–420.
(68) Jakubowski, W.; Tsarevsky, N. V.; Higashihara, T.; Faust, R.; Matyjaszewski, K. *Macromolecules* **2008**, *41*, 2318–2323.

Table 2. Values of Free Energies (ΔG) and Equilibrium Constants (K_{RX}) for Bond Homolysis, Halogenophilicities ($K_{Cu,X\bullet}$), and ATRP Equilibrium Constants (K_{ATRP}) in Acetonitrile at 22 °C

ligand	initiator	ΔG (kcal mol^{-1}) [a]	log K_{RX} [b]	log K_{ATRP} [c]	log $K_{Cu,X\bullet}$ [d]	log K_{ATRP} − log $K_{Cu,X\bullet}$
NPPMI	EtBriB	50.49	−37.38	−10.3	27.08	−37.38
NPPMI	EBPA	45.21	−33.47	−6.32	27.08	−33.40
bpy	EtBriB	50.49	−37.38	−8.41	28.97	−37.38
bpy	PEBr	52.61	−38.95	−9	28.97	−37.97
HMTETA	EtBriB	50.49	−37.38	−7.96	29.42	−37.38
HMTETA	BrAN	50.75	−37.57	−8.54	29.42	−37.96
HMTETA	BrPN	48.31	−35.77	−7.1	29.42	−36.52
HMTETA	PEBr	52.61	−38.95	−8.54	29.42	−37.96
PMDETA	EtBriB	50.49	−37.38	−7.12	30.26	−37.38
PMDETA	BrAN	50.75	−37.57	−5.06	30.26	−35.32
PMDETA	BrPN	48.31	−35.77	−6.23	30.26	−36.49
PMDETA	MBrP	52.70	−39.02	−8.40	30.26	−38.66
PMDETA	PEBr	52.61	−38.95	−7.48	30.26	−37.74
TPMA	EtBriB	50.49	−37.38	−5.02	32.36	−37.38
TPMA	BrAN	50.75	−37.57	−4.25	32.36	−36.61
TPMA	BrPN	48.31	−35.77	−3.96	32.36	−36.32
TPMA	MBrAc	54.86	−40.62	−6.49	32.36	−38.85
TPMA	MBrP	52.70	−39.02	−6.49	32.36	−38.85
TPMA	BzBr	52.75	−39.06	−6.17	32.36	−38.53
TPMA	PEBr	52.61	−38.95	−5.34	32.36	−37.70
Me_6TREN	EtBriB	50.49	−37.38	−3.82	33.56	−37.38
Me_6TREN	MBrAc	54.86	−40.62	−4.66	33.56	−38.22
Me_6TREN	MBrP	52.70	−39.02	−5.54	33.56	−39.10
Me_6TREN	BzBr	52.75	−39.06	−6.08	33.56	−39.64
Me_6TREN	PEBr	52.61	−38.95	−3.59	33.56	−37.15
bpy	EtCliB	64.49	−47.75	−9.22	38.53	−47.75
bpy	ECPA	58.76	−43.51	−6.48	38.53	−45.01
TPMA	EtCliB	64.49	−47.75	−5.83	41.92	−47.75
TPMA	ClAN	63.60	−47.09	−4.51	41.92	−46.43
TPMA	ClPN	61.71	−45.69	−4.66	41.92	−46.58
TPMA	MClAc	66.18	−49.00	−6.38	41.92	−48.30
TPMA	MClP	66.44	−49.19	−7.38	41.92	−49.30
TPMA	BzCl	65.88	−48.78	−6.35	41.92	−48.27
TPMA	PECl	65.01	−48.14	−6.07	41.92	−47.99
Me_6TREN	EtCliB	64.49	−47.75	−4.64	43.11	−47.75
Me_6TREN	MClAc	66.18	−49.00	−5.46	43.11	−48.57
Me_6TREN	MClP	66.44	−49.19	−5.7	43.11	−48.81
Me_6TREN	BzCl	65.88	−48.78	−5.44	43.11	−48.55
Me_6TREN	PECl	65.01	−48.14	−4.85	43.11	−47.96

[a] Values taken from ref 45. [b] Calculated from corresponding calculated values of ΔG. [c] Experimentally determined. [d] Calculated for each catalyst using EtBriB and/or EtCliB as the reference compound according to the equation log $K_{Cu,X\bullet}$ = log K_{ATRP} − log K_{RX}.

Most of the extrapolated values are close to the measured values (within a factor of 2). It is possible that some additional special effects can influence the selectivities of catalysts or initiators. For example, steric effects may give a special contribution for tertiary species. Some functional groups (such as amide or unsaturation) may interact with the catalyst. Alkyl halides with strong electron affinities may directly undergo OSET, and the resulting radicals may be reduced to anions.[7] An independent project to investigate the selectivities of ligands and initiators is underway. Nevertheless, the extrapolated values of K_{ATRP} should be useful for a rough estimation of the activity of a particular catalyst/initiator system.

The rate of ATRP depends strongly on the value of K_{ATRP} (eq 1). However, control of polymerization (e.g., polydispersity) depends on the values of deactivation rate constant k_{deact} (eq 2). Direct measurements of k_{deact} are difficult, since the rate constants are very large, approaching diffusion-controlled values. They were previously determined for model compounds using "clock" reactions[6] and for macromolecular species from initial degrees of polymerization[25] or evolution of polydispersity with conversion.[24] However, the k_{deact} values could be calculated directly from the ratio k_{act}/K_{ATRP}. We have previously reported k_{act} values for a wide range of ligands and catalysts at 35 °C in acetonitrile. In this work, we have determined the ATRP equilibrium constants for a similar range of initiators and catalysts at 22 °C. Values of k_{act} show a moderate dependence on temperature. As shown in Table 4, values of k_{act} increase on average by a factor of 2 as the temperature increases from 22 to 35 °C.

We realize that activation energies for k_{act} can be affected by the structure of ligands and initiators; however, for simplicity, we use the average value of the correcting ratio (0.5) to convert the values of k_{act} from 35 to 22 °C. Values of K_{ATRP}, k_{act}, and k_{deact} in acetonitrile at 22 °C calculated in this way are listed in Table 5. Values in red are extrapolated values, which were discussed in previous reports[17,18] and also in this study. Some of the K_{ATRP} and k_{deact} values are not yet available because the reactions are either

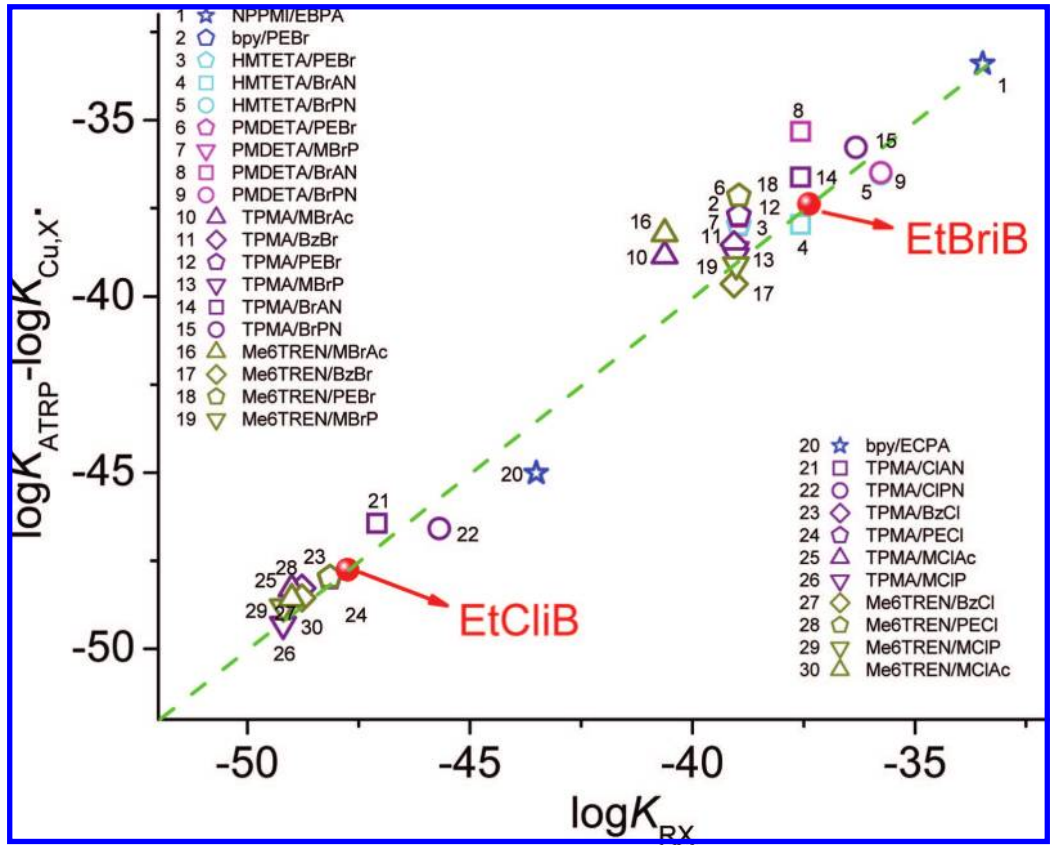

Figure 4. Correlation of K_{RX} values calculated from K_{ATRP} using constant halogenophilicities for various complexes with values calculated from free energies of homolytic bond dissociation for alkyl halides. Values of log K_{RX} correspond to calculated values of ΔG,[45] values of log K_{ATRP} were experimentally determined, and values of log $K_{Cu,X}$· were calculated for each catalyst using EtBriB and/or EtCliB as the reference compound according to the equation log $K_{Cu,X\cdot}$ = log K_{ATRP} − log K_{RX}.

Table 3. Comparison of Extrapolated and Measured K_{ATRP} Values

no.	ligand	initiator	K_{ATRP} (measured)[a]	K_{ATRP} (extrap.)[b]	K_{ATRP} ratio (extrap./measured)
1	Me_6TREN	MClAc	3.5×10^{-6}	6.6×10^{-6}	1.88
2	Me_6TREN	BzCl	3.6×10^{-6}	7.0×10^{-6}	1.95
3	Me_6TREN	PECl	1.4×10^{-5}	1.3×10^{-5}	0.96
4	Me_6TREN	MClP	2.0×10^{-6}	5.9×10^{-7}	0.30
5	Me_6TREN	MBrAc	2.2×10^{-5}	5.0×10^{-6}	0.23
6	Me_6TREN	BzBr	2.8×10^{-5}	1.1×10^{-5}	0.39
7	Me_6TREN	tBBrP	8.4×10^{-7}	6.6×10^{-7}	0.78
8	Me_6TREN	PEBr	2.6×10^{-4}	7.2×10^{-5}	0.28
9	Me_6TREN	MBrP	2.9×10^{-6}	5.0×10^{-6}	1.72
10	bpy	PEBr	1.0×10^{-9}	1.9×10^{-9}	1.90
11	bpy	AllBr	3.0×10^{-9}	7.0×10^{-9}	2.33
12	PMDETA	PEBr	3.3×10^{-8}	3.6×10^{-8}	1.10
13	PMDETA	MBrP	4.0×10^{-9}	3.0×10^{-9}	0.75
14	PMDETA	BrPN	5.9×10^{-7}	8.6×10^{-7}	1.46
15	HMTETA	PEBr	2.9×10^{-9}	5.3×10^{-9}	1.83
16	HMTETA	PECl	7.9×10^{-10}	9.9×10^{-9}	1.25
17	HMTETA	BrAN	7.9×10^{-8}	6.4×10^{-8}	0.84
18	HMTETA	BrPN	3.2×10^{-8}	1.3×10^{-7}	4.06

[a] Values were measured at 22 °C in MeCN.[30,44,54,68] [b] Values were extrapolated using the following calculation: K_{ATRP}(Cu^I/ligand with initiator) = K_{ATRP} (Cu^IBr/ligand with EtBriB) × K_{ATRP}(Cu^I/TPMA with initiator)/(Cu^IBr/TPMA with EtBriB) (see Table 5).

too slow or too fast to carry out at present. The values extrapolated from the reference catalyst and initiators are expected to be close to the experimental data, as demonstrated for some extrapolated and measured values of k_{act}[18] and K_{ATRP}. Thus, the table not only enables a fast comparison of activities for catalysts and initiators in ATRP but also provides good direction for future development of new ligands and identifies limitations for the use of new

Table 4. Comparison of Activation Rate Constant Values at 22 and 35 °C

no.	ligand	initiator	k_{act} (22 °C)	k_{act} (35 °C)	k_{act} ratio (35 °C/25 °C)
1	NPPMI	EtBriB	1.2×10^{-3}	2.4×10^{-3}	2.0
2	bpy	EtBriB	0.04	0.066	1.6
3	bpy	PEBr	4.5×10^{-3}	0.010	2.2
4	HMTETA	EtBriB	0.06	0.14	2.3
5	PMDETA	MBrP	0.17	0.33	1.9

monomers and initiators. Nevertheless, all of the extrapolated values should be taken with a large degree of caution because of the assumption of constant selectivity as well as the neglect of variations in the activation energy. Larger errors might happen for some very active systems because of the extrapolation over several orders of magnitude; for example, the extrapolated ratio of K_{ATRP} for EBPA and ECPA with TPMA ligand was $\sim 10^2$, but direct measurements of K_{ATRP} for several alkyl bromides and chlorides gave a ratio ≤ 10.

It should be noted that both thermodynamic and kinetic parameters depend on temperature and solvent. Detailed investigations of temperature and solvent effects on k_{act}, k_{deact}, and K_{ATRP} are currently being carried out in our laboratories.

Summary of Structural Effects in Catalyst and Initiator on k_{act}, k_{deact} and K_{ATRP}. This final section attempts to demonstrate how the structure of the ligands complexing to Cu, together with the initiators used, affects ATRP in terms of k_{act}, k_{deact}, and K_{ATRP}.

Figure 5 shows that ATRP equilibrium constants increase as a result of both increases in k_{act} and decreases in k_{deact} and that k_{act}

Table 5. Activation Rate Constants (k_{act}), Deactivation Rate Constants (k_{deact}), and Equilibrium Constants (K_{ATRP}) at 22 °C in Acetonitrile Extrapolated Using the Constant Selectivity Principle[a]

		MClAc	BzCl	PECl	MClP	AllCl	AllBr	EtCliB	MBrAc	tBBrP	BzBr	ClAN	PEBr	MBrP	ClPN	MIP	MBriB	EtBriB	BrAN	BrPN	ECPA	EBPA
N4[2,3,2]	k_{act}	3.6E-7	1.2E-6	2.2E-6	3.3E-6	2.5E-7	8.6E-6	4.9E-6	6.7E-6	1.9E-5	2.2E-5	3.0E-5	3.8E-5	7.3E-5	1.0E-4	1.2E-4	5.8E-4	6.0E-4	1.6E-3	5.1E-3	3.1E-2	1.2E+0
	k_{deact}	1.9E+4	6.2E+4	5.9E+4	2.0E+6	2.4E+3	1.1E+4	7.6E+4	4.8E+5	1.7E+7	1.2E+7	2.2E+4	1.9E+5	5.2E+6	1.1E+5	1.2E+8	7.3E+5	1.4E+6	6.4E+5	1.1E+6	8.6E+5	2.9E+5
	K_{ATRP}	1.8E-11	2.0E-11	3.8E-11	1.7E-12	1.0E-10	7.5E-10	6.4E-11	1.4E-11	1.1E-12	1.8E-12	1.4E-9	2.0E-10	1.4E-11	9.6E-10	9.6E-13	7.9E-10	4.2E-10	2.5E-9	4.8E-9	3.6E-8	4.0E-6
PMI	k_{act}	7.1E-7	2.4E-6	4.4E-6	6.7E-6	5.0E-7	1.7E-5	9.8E-6	1.3E-5	3.8E-5	4.4E-5	6.0E-5	7.6E-5	1.5E-4	2.0E-4	2.4E-4	1.2E-3	1.2E-3	3.2E-3	1.0E-2	6.2E-2	2.4E+0
	k_{deact}	3.3E+5	1.0E+6	9.9E+5	3.0E+7	4.1E+4	1.9E+5	1.3E+6	8.0E+6	2.8E+8	1.3E+7	3.7E+5	3.2E+6	8.8E+7	1.8E+6	2.1E+9	1.2E+7	2.4E+7	1.1E+7	1.8E+7	1.5E+7	4.9E+6
	K_{ATRP}	2.2E-12	2.3E-12	4.5E-12	2.2E-13	1.2E-11	9.0E-11	7.7E-12	1.7E-12	1.4E-13	3.5E-12	1.6E-10	2.4E-11	1.7E-12	1.1E-10	1.1E-13	9.4E-11	5.0E-11	2.9E-10	5.7E-10	4.3E-9	4.8E-7
N4[3,2,3]	k_{act}	1.5E-6	5.1E-6	9.3E-6	1.4E-5	1.0E-6	3.6E-5	2.0E-5	2.8E-5	7.9E-5	9.3E-5	1.3E-4	1.6E-4	3.1E-4	4.3E-4	4.9E-4	2.4E-3	0.003	6.6E-3	2.1E-2	1.3E-1	4.9E+0
	k_{deact}	1.1E+4	3.4E+4	3.2E+4	9.9E+5	1.3E+3	6.2E+3	4.2E+4	2.6E+5	9.1E+6	4.1E+5	1.2E+4	1.0E+5	2.9E+6	5.8E+4	6.7E+7	4.0E+5	7.8E+5	3.5E+5	5.8E+5	4.7E+5	1.6E+5
	K_{ATRP}	1.4E-10	1.5E-10	2.9E-10	1.4E-11	7.8E-10	5.7E-9	4.9E-10	1.1E-10	8.7E-12	2.3E-10	1.0E-8	1.5E-9	1.1E-10	7.3E-9	7.3E-12	6.0E-9	3.2E-9	1.9E-8	3.7E-8	2.7E-7	3.1E-5
AN_6TREN	k_{act}	7.1E-6	2.4E-5	4.4E-5	6.7E-5	5.0E-6	1.7E-4	9.8E-5	1.3E-4	3.8E-4	4.4E-4	6.0E-4	7.6E-4	1.5E-3	2.0E-3	2.4E-3	1.2E-2	0.012	3.2E-2	1.0E-1	6.2E-1	2.4E+1
	k_{deact}	9.6E+4	3.1E+5	2.9E+5	9.0E+6	1.2E+4	5.6E+4	3.8E+5	2.4E+6	8.2E+7	3.7E+6	1.1E+5	9.3E+5	2.6E+7	5.2E+5	6.0E+8	3.6E+6	7.1E+6	3.2E+6	5.3E+6	4.3E+6	1.4E+6
	K_{ATRP}	7.4E-11	8.0E-11	1.5E-10	7.4E-12	4.1E-10	3.0E-9	2.6E-10	5.7E-11	4.6E-12	1.2E-10	5.5E-9	8.1E-10	5.7E-11	3.9E-9	3.9E-12	3.2E-9	1.7E-9	9.9E-9	1.9E-8	1.5E-7	1.6E-5
Et_6TREN	k_{act}	2.6E-5	9.0E-5	1.6E-4	2.4E-4	1.8E-5	6.3E-4	3.6E-4	4.9E-4	1.4E-3	1.6E-3	2.2E-3	2.8E-3	5.4E-3	7.5E-3	8.6E-3	4.2E-2	0.044	1.2E-1	3.8E-1	2.3E+0	8.6E+1
	k_{deact}	6.3E+5	2.0E+6	1.9E+6	5.9E+7	8.0E+4	3.7E+5	2.5E+6	1.6E+7	5.4E+8	2.4E+7	7.3E+5	6.2E+6	1.7E+8	3.5E+6	4.0E+9	2.4E+7	4.7E+7	2.1E+7	3.5E+7	2.8E+7	9.6E+6
	K_{ATRP}	4.1E-11	4.4E-11	8.4E-11	4.1E-12	2.3E-10	1.7E-9	1.4E-10	3.1E-11	2.5E-12	6.7E-11	3.0E-9	4.5E-10	3.1E-11	2.2E-9	2.2E-12	1.8E-9	9.4E-10	5.5E-9	1.1E-8	8.0E-8	9.0E-6
bpy	k_{act}	2.0E-5	6.7E-5	1.2E-4	1.8E-4	1.4E-5	4.7E-4	2.7E-4	3.7E-4	1.0E-3	1.2E-3	1.7E-3	2.1E-3	4.0E-3	5.6E-3	6.5E-3	3.2E-2	0.033	8.7E-2	2.8E-1	1.7E+0	6.5E+1
	k_{deact}	1.1E+5	3.7E+5	3.5E+5	1.1E+7	1.4E+4	1.6E+5	4.5E+5	2.8E+6	9.8E+7	4.4E+6	1.3E+5	2.1E+6	3.1E+7	6.3E+5	7.2E+8	4.3E+6	8.5E+6	3.8E+6	6.3E+6	5.1E+6	1.7E+6
	K_{ATRP}	1.7E-10	1.8E-10	3.5E-10	1.7E-11	9.5E-10	3.0E-9	6.0E-10	1.3E-10	1.1E-11	2.8E-10	1.3E-8	1.0E-9	1.3E-10	8.9E-9	8.9E-12	7.3E-9	3.9E-9	2.3E-8	4.5E-8	3.3E-7	3.7E-5
HMTETA	k_{act}	4.1E-5	1.4E-4	2.6E-4	3.9E-4	2.9E-5	1.0E-3	5.7E-4	7.8E-4	2.2E-3	2.6E-3	3.5E-3	4.4E-3	8.6E-3	1.2E-2	1.4E-2	6.7E-2	0.07	1.8E-1	6.0E-1	3.6E+0	1.4E+2
	k_{deact}	8.6E+4	2.8E+5	2.6E+5	8.1E+6	1.1E+4	5.1E+4	3.4E+5	2.1E+6	7.4E+7	3.3E+6	9.9E+4	1.5E+6	2.3E+7	4.7E+5	5.5E+8	3.3E+6	6.4E+6	2.3E+6	1.9E+7	3.8E+6	1.3E+6
	K_{ATRP}	4.8E-10	5.2E-10	9.9E-10	4.8E-11	2.7E-9	2.0E-8	1.7E-9	3.7E-10	3.0E-11	7.8E-10	3.6E-8	2.9E-9	3.7E-10	2.5E-8	2.5E-11	2.1E-8	1.1E-8	7.9E-8	3.2E-8	9.4E-7	1.1E-4
BPMPA	k_{act}	5.9E-5	2.0E-4	3.7E-4	5.6E-4	4.1E-5	1.4E-3	8.1E-4	1.1E-3	3.1E-3	3.7E-3	5.0E-3	6.3E-3	1.2E-2	1.7E-2	2.0E-2	9.6E-2	0.10	2.6E-1	8.6E-1	5.2E+0	2.0E+2
	k_{deact}	2.2E+4	7.0E+4	6.7E+4	2.0E+6	2.7E+3	1.3E+4	8.6E+4	5.4E+5	1.9E+7	8.4E+5	2.5E+4	2.1E+5	5.9E+6	1.2E+5	1.4E+8	8.3E+5	1.6E+6	7.3E+5	1.2E+6	9.8E+5	3.3E+5
	K_{ATRP}	2.7E-9	2.9E-9	5.6E-9	2.7E-10	1.5E-8	1.1E-7	9.5E-9	2.1E-9	1.7E-10	4.4E-9	2.0E-7	3.0E-8	2.1E-9	1.4E-7	1.4E-10	1.2E-7	6.2E-8	3.6E-7	7.1E-7	5.3E-6	6.0E-4
N4[2,2,3]	k_{act}	7.1E-5	2.4E-4	4.4E-4	6.7E-4	5.0E-5	1.7E-3	9.8E-4	1.3E-3	3.8E-3	4.4E-3	6.0E-3	7.6E-3	1.5E-2	2.0E-2	2.4E-2	1.2E-1	0.12	3.2E-1	1.0E+0	6.2E+0	2.4E+2
	k_{deact}	1.1E+4	3.5E+4	3.3E+4	1.0E+6	1.4E+3	6.4E+3	4.3E+4	2.7E+5	9.3E+6	4.2E+5	1.2E+4	1.1E+5	2.9E+6	5.9E+4	6.9E+7	4.1E+5	8.0E+5	3.6E+5	6.0E+5	4.8E+5	1.6E+5
	K_{ATRP}	6.6E-9	7.0E-9	1.3E-8	6.6E-10	3.7E-8	2.7E-7	2.3E-8	5.0E-9	4.1E-10	1.1E-8	4.8E-7	7.2E-8	5.0E-9	3.4E-7	3.4E-10	2.8E-7	1.5E-7	8.8E-7	1.7E-6	1.3E-5	1.4E-3
dNbpy	k_{act}	1.8E-4	6.1E-4	1.1E-3	1.7E-3	1.2E-4	4.3E-3	2.4E-3	3.3E-3	9.4E-3	1.1E-2	1.5E-2	1.9E-2	3.7E-2	5.1E-2	5.9E-2	2.9E-1	0.3	7.9E-1	2.6E+0	1.5E+1	5.9E+2
	k_{deact}	1.4E+5	4.3E+5	4.1E+5	1.3E+7	1.7E+4	8.0E+4	5.3E+5	3.3E+6	1.2E+8	5.2E+6	1.6E+5	1.3E+6	3.7E+7	7.4E+5	8.6E+8	5.1E+6	1.0E+7	4.5E+6	7.5E+6	6.0E+6	2.0E+6
	K_{ATRP}	1.3E-9	1.4E-9	2.7E-9	1.3E-10	7.3E-9	5.4E-8	4.6E-9	1.0E-9	8.1E-11	2.1E-9	9.7E-8	1.4E-8	1.0E-9	6.9E-8	6.9E-11	5.6E-8	3.0E-8	1.8E-7	3.4E-7	2.6E-6	2.9E-4
$Me_4Cyclam$	k_{act}	2.0E-4	6.9E-4	1.3E-3	1.9E-3	1.4E-4	4.9E-3	2.8E-3	3.8E-3	1.1E-2	1.3E-2	1.7E-2	2.1E-2	4.2E-2	5.8E-2	6.7E-2	3.3E-1	0.34	8.9E-1	2.9E+0	1.8E+1	6.7E+2
	k_{deact}	9.8E+1	3.1E+2	3.0E+2	9.2E+3	1.2E+1	5.8E+1	3.8E+2	2.4E+3	8.4E+4	3.8E+3	1.1E+2	9.5E+2	2.7E+4	5.4E+2	6.2E+5	3.7E+3	7.2E+3	3.3E+3	5.4E+3	4.4E+3	1.5E+3
	K_{ATRP}	2.1E-6	2.2E-6	4.2E-6	2.1E-7	1.1E-5	8.4E-5	7.2E-6	1.6E-6	1.3E-7	3.3E-6	1.5E-4	2.3E-5	1.6E-6	1.1E-4	1.1E-7	8.8E-5	4.7E-5	2.7E-4	5.4E-4	4.0E-3	4.5E-1
MA_6TREN	k_{act}	3.7E-4	1.3E-3	2.3E-3	3.4E-3	2.6E-4	8.9E-3	5.1E-3	6.9E-3	2.0E-2	2.3E-2	3.1E-2	3.9E-2	7.6E-2	1.1E-1	1.2E-1	6.0E-1	0.62	1.6E+0	5.3E+0	3.2E+1	1.2E+3
	k_{deact}	4.9E+5	1.6E+6	1.5E+6	4.6E+7	6.2E+4	2.9E+5	1.9E+6	1.2E+7	4.2E+8	1.9E+7	5.7E+5	4.8E+6	1.3E+8	2.7E+6	3.1E+9	1.9E+7	3.6E+7	1.6E+7	2.7E+7	2.2E+7	7.5E+6
	K_{ATRP}	7.4E-10	8.0E-10	1.5E-9	7.4E-11	4.1E-9	3.0E-8	2.6E-9	5.7E-10	4.6E-11	1.2E-9	5.5E-8	8.1E-9	5.7E-10	3.9E-8	3.9E-11	3.2E-8	1.7E-8	9.9E-8	1.9E-7	1.5E-6	1.6E-4

Table 5. Continued

		MClAc	BzCl	PECl	MClP	AllCl	AllBr	EtCliB	MBrAc	tBBrP	BzBr	ClAN	PEBr	MBrP	ClPN	MIP	MBriB	EtBriB	BrAN	BrPN	ECPA	EBPA
PMDETA	k_{act}	8.3E-4	2.9E-3	5.2E-3	7.8E-3	5.8E-4	2.0E-2	1.1E-2	1.6E-2	4.4E-2	5.2E-2	7.1E-2	8.8E-2	1.7E-1	2.4E-1	2.7E-1	1.3E+0	1.4	3.7E+0	1.2E+1	7.2E+1	2.7E+3
	k_{deact}	2.5E+5	8.1E+5	7.7E+5	2.4E+7	3.2E+4	1.5E+5	9.9E+5	6.2E+6	2.2E+8	9.8E+6	2.9E+5	2.7E+6	4.3E+7	1.4E+6	1.6E+9	9.6E+6	1.9E+7	4.2E+5	2.0E+7	1.1E+7	3.8E+6
	K_{ATRP}	3.3E-9	3.5E-9	6.7E-9	3.3E-10	1.8E-8	1.3E-7	1.2E-8	2.5E-9	2.0E-10	5.3E-9	2.4E-7	3.3E-8	4.0E-9	1.7E-7	1.7E-10	1.4E-7	7.5E-8	8.8E-6	5.9E-7	6.4E-6	7.2E-4
BA_6TREN	k_{act}	1.2E-3	4.2E-3	7.6E-3	1.1E-2	8.5E-4	2.9E-2	1.7E-2	2.3E-2	6.5E-2	7.6E-2	1.0E-1	1.3E-1	2.5E-1	3.5E-1	4.0E-1	2.0E+0	2.05	5.4E+0	1.8E+1	1.1E+2	4.0E+3
	k_{deact}	5.3E+5	1.7E+6	1.6E+6	5.0E+7	6.7E+4	3.1E+5	2.1E+6	1.3E+7	4.6E+8	2.1E+7	6.1E+5	5.2E+6	1.4E+8	2.9E+6	3.4E+9	2.0E+7	3.9E+7	1.8E+7	2.9E+7	2.4E+7	8.1E+6
	K_{ATRP}	2.3E-9	2.4E-9	4.7E-9	2.3E-10	1.3E-8	9.3E-8	8.0E-9	1.7E-9	1.4E-10	3.7E-9	1.7E-7	2.5E-8	1.7E-9	1.2E-7	1.2E-10	9.8E-8	5.2E-8	3.0E-7	6.0E-7	4.4E-6	5.0E-4
BPED	k_{act}	1.3E-3	4.5E-3	8.3E-3	1.2E-2	9.2E-4	3.2E-2	1.8E-2	2.5E-2	7.0E-2	8.3E-2	1.1E-1	1.4E-1	2.7E-1	3.8E-1	4.4E-1	2.1E+0	2.23	5.9E+0	1.9E+1	1.2E+2	4.4E+3
	k_{deact}	2.7E+3	8.8E+3	8.4E+3	2.6E+5	3.4E+2	1.6E+3	1.1E+4	6.8E+4	2.4E+6	1.1E+5	3.2E+3	2.7E+4	7.4E+5	1.5E+4	1.7E+7	1.0E+5	2.0E+5	9.1E+4	1.5E+5	1.2E+5	4.1E+4
	K_{ATRP}	4.8E-7	5.2E-7	9.9E-7	4.8E-8	2.7E-6	2.0E-5	1.7E-6	3.7E-7	3.0E-8	7.8E-7	3.6E-5	5.3E-6	3.7E-7	2.5E-5	2.5E-8	2.1E-5	1.1E-5	6.4E-5	1.3E-4	9.4E-4	1.1E-1
TPEDA	k_{act}	3.2E-3	1.1E-2	2.0E-2	3.0E-2	2.2E-3	7.7E-2	4.4E-2	6.0E-2	1.7E-1	2.0E-1	2.7E-1	3.4E-1	6.6E-1	9.2E-1	1.1E+0	5.2E+0	5.4	1.4E+1	4.6E+1	2.8E+2	1.1E+4
	k_{deact}	3.7E+4	1.2E+5	1.1E+5	3.4E+6	4.6E+3	2.2E+4	1.4E+5	9.0E+5	3.1E+7	1.4E+6	4.2E+4	3.5E+5	9.9E+6	2.0E+5	2.3E+8	1.4E+6	2.7E+6	1.2E+6	2.0E+6	1.6E+6	5.5E+5
	K_{ATRP}	8.8E-8	9.4E-8	1.8E-7	8.8E-9	4.9E-7	3.6E-6	3.1E-7	6.7E-8	5.4E-9	1.4E-7	6.5E-6	9.6E-7	6.7E-8	4.6E-6	4.6E-9	3.8E-6	2.0E-6	1.2E-5	2.3E-5	1.7E-4	1.9E-2
TPMA	k_{act}	1.8E-2	6.4E-2	1.2E-1	1.7E-1	1.3E-2	4.5E-1	2.5E-1	3.5E-1	9.8E-1	1.2E+0	1.6E+0	2.0E+0	3.8E+0	5.3E+0	6.1E+0	3.0E+1	31.2	8.2E+1	2.7E+2	1.6E+3	6.1E+4
	k_{deact}	4.4E+4	1.4E+5	1.3E+5	4.1E+6	5.5E+3	2.6E+4	1.7E+5	1.1E+6	3.8E+7	1.7E+6	5.1E+4	4.3E+5	1.2E+7	2.4E+5	2.8E+8	1.7E+6	3.3E+6	1.5E+6	2.4E+6	2.0E+6	6.6E+5
	K_{ATRP}	4.2E-7	4.5E-7	8.6E-7	4.2E-8	2.3E-6	1.7E-5	1.5E-6	3.2E-7	2.6E-8	6.8E-7	3.1E-5	4.6E-6	3.2E-7	2.2E-5	2.2E-8	1.8E-5	9.6E-6	5.6E-5	1.1E-4	8.2E-4	9.2E-2
Me_6TREN	k_{act}	1.3E-1	4.6E-1	8.4E-1	1.3E+0	9.4E-2	3.3E+0	1.9E+0	2.5E+0	7.2E+0	8.4E+0	1.1E+1	1.4E+1	2.8E+1	3.9E+1	4.5E+1	2.2E+2	227.8	6.0E+2	1.9E+3	1.2E+4	4.5E+5
	k_{deact}	3.9E+4	1.3E+5	6.0E+4	6.3E+5	2.6E+3	1.2E+4	8.1E+4	1.2E+5	1.8E+7	1.0E+7	2.4E+4	5.5E+4	9.6E+6	1.1E+5	1.3E+8	7.8E+5	1.5E+6	6.8E+5	1.1E+6	9.2E+5	3.1E+5
	K_{ATRP}	3.5E-6	3.6E-6	1.4E-5	2.0E-6	3.7E-5	2.7E-4	2.3E-5	2.2E-5	4.1E-7	8.4E-7	4.8E-4	2.6E-4	2.9E-6	3.4E-4	3.4E-7	2.8E-4	1.5E-4	8.8E-4	1.7E-3	1.3E-2	1.4E+0
Cyclam-B	k_{act}	2.1E-1	7.2E-1	1.3E+0	2.0E+0	1.5E-1	5.1E+0	2.9E+0	3.9E+0	1.1E+1	1.3E+1	1.8E+1	2.2E+1	4.3E+1	6.0E+1	7.0E+1	3.4E+2	354.4	9.3E+2	3.0E+3	1.8E+4	7.0E+5
	k_{deact}	2.1E+3	6.7E+3	6.4E+3	2.0E+5	2.6E+2	1.2E+3	8.2E+3	5.1E+4	1.8E+6	8.1E+4	2.4E+3	2.0E+4	5.6E+5	1.1E+4	1.3E+7	7.9E+4	1.5E+5	6.9E+4	1.2E+5	3.2E+4	3.2E+4
	K_{ATRP}	9.9E-5	1.1E-4	2.1E-4	1.0E-5	5.6E-4	4.1E-3	3.5E-4	7.7E-5	6.2E-6	1.6E-4	7.4E-3	1.1E-3	7.7E-5	5.3E-3	5.3E-6	4.3E-3	4.3E-3	1.3E-2	2.6E-2	4.3E-3	4.3E-3

[a] Values in black were measured in MeCN at 22 °C, values in red were extrapolated from those for the reference catalysts and initiators, and values in green are k_{act} values extrapolated from the corresponding values at 35 °C.[18] Values of k_{act} and k_{deact} have units of M^{-1} s^{-1}.

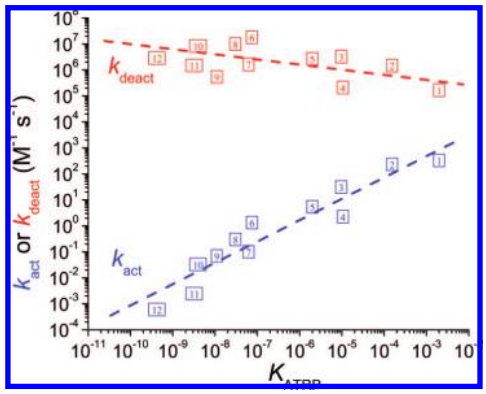

Figure 5. Correlation of k_{act} and k_{deact} with K_{ATRP} for various $Cu^{I}Br$/ligand catalysts with EtBriB at 22 °C in MeCN (the broken lines are just to guide the reader's eye). The k_{act} values were extrapolated from those at 35 °C.[16,17] Ligand number key: (1) Cyclam-B; (2) Me_6TREN; (3) TPMA; (4) BPED; (5) TPEDA; (6) PMDETA; (7) BPMPA; (8) dNbpy; (9) HMTETA; (10) bpy; (11) N4[3,2,3]; (12) N4[2,3,2].

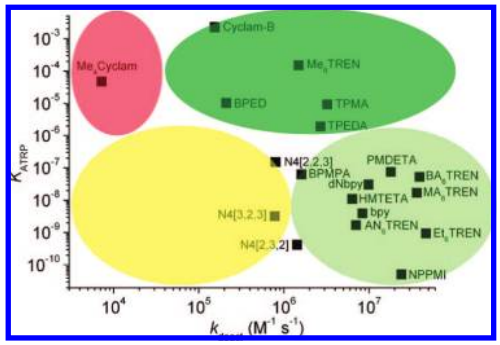

Figure 6. Correlation of K_{ATRP} and k_{deact} for various Cu^{I}/ligand catalysts with EtBriB at 22 °C in MeCN (see Table 5).

contributes to the overall value of K_{ATRP} much more than k_{deact}. Figure 5 also shows that stronger activators are generally weaker deactivators.

However, the "ideal" ATRP catalyst should have a large value of K_{ATRP} (so it can be used at low concentrations) but also should have a large value of k_{deact} (to provide good control and generate polymers with low polydispersity). Such catalysts would be ideal for activators regenerated by electron transfer (ARGET) and initiators for continuous activator regeneration (ICAR) methods of ATRP, which are carried out with parts per million amounts of Cu.[26,27] Figure 6 shows the more-detailed correlation of K_{ATRP} and k_{deact} for all of the ligands discussed in this report. The ligands in this "map" for rational ligand selection are divided into four types. The ligands in the lower-right section of the map are typical ligands used in ATRP that give moderately fast polymerization with fairly large K_{ATRP} values and good control due to sufficiently large k_{deact} values. Most traditional ATRP ligands, such as bpy, dNbpy, PMDETA and HMTETA, fall within this area. The ligands in the upper-right area are a new generation of ligands that afford both very fast polymerization with large K_{ATRP} values and good control with fairly large k_{deact} values. These ligands have been successfully used in new ATRP systems such as ICAR ATRP and ARGET ATRP. Ligands in the lower-left part can form catalysts that give rise to slow rates of polymerization and poor control due to small K_{ATRP} and k_{deact} values, respectively. These are inefficient ligands for ATRP, and therefore, only a few of them, such as N4[3,2,3] and N[2,3,2], are included in this report. Although ligands in the upper-left section of the map (e.g., Me_4Cyclam) can form catalysts that afford very fast polymerization with large K_{ATRP} values, the polymerization is uncontrolled because of the small values of k_{deact}.

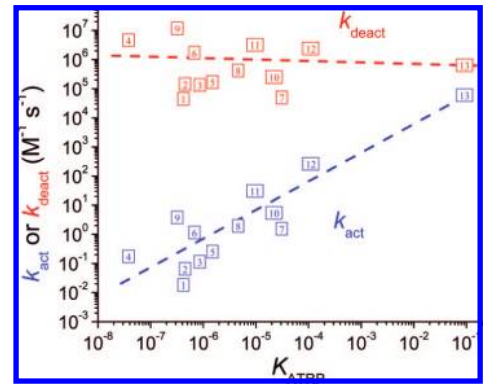

Figure 7. Correlation of k_{act} and k_{deact} with K_{ATRP} for Cu^{I}/TPMA with various initiators at 22 °C in MeCN (the broken lines are just to guide the reader's eye). The k_{act} values were extrapolated from those at 35 °C.[16,18] Initiator number key: (1) MClAc; (2) BzCl; (3) PECl; (4) MClP; (5) EtCliB; (6) BzBr; (7) ClAN; (8) PEBr; (9) MBrP; (10) ClPN; (11) EtBriB; (12) BrPN; (13) EBPA.

The trend in Figure 7 for initiators is similar to that in Figure 5. The more-reactive dormant species (larger k_{act}) form more-stable, i.e., less-reactive radicals (smaller k_{deact}). The initiators that have larger K_{ATRP} values also have larger k_{act} and smaller k_{deact} values. However, k_{deact} is much less dependent on K_{ATRP} for initiators than for ligands. This suggests a smaller radical selectivity toward Cu^{II} species.

Conclusions

Equilibrium constants for catalysts with various nitrogen-based ligands and alkyl halide-based initiators have been determined in acetonitrile at 22 °C. The activities of the Cu^{I}/ligands and initiators span 7 orders of magnitude and are strongly affected by the structures of the ligand and the initiator. In general, the activity of the Cu complex decreases as the ligand is changed from Cyclam-B > N4-branched > N4-linear > N3 > N2. The ethylene group provides a better linkage than the propylene group for the coordinating nitrogens in the ligand. The activity of the initiator decreases as the alkyl group is varied from 3° > 2° > 1° and its α-substituent varied from −CN < −Ph < −C(O)OR > $-CH_3$. In general, the activities of alkyl bromide initiators are several times larger than those of the corresponding chlorides. A full kinetic picture for ATRP was constructed in order to comprehensively understand the structure−activity relationships for the ligand and initiators in ATRP. Along with the excellent correlation between $Cu^{II/I}$ redox potentials and equilibrium constants, it is possible to design and predict the activities of some new ATRP catalytic and initiating systems.

Acknowledgment. Financial support from the NSF (CHE-07-15494) and the CRP Consortium at CMU is gratefully acknowledged. M.L.C. gratefully acknowledges financial support from the Australian Research Council under their Centres of Excellence program.

Supporting Information Available: Complete ref 49. This material is available free of charge via the Internet at http://pubs.acs.org.

JA802290A